Fabrication and characterization of high-damage resistance Zn-diffused MgO: PPLN ridge waveguides*

CHENG Xing[1,2,3], FENG Xinkai[2,3], MA Lei[2,3], CHEN Jiaying[2,3], CHEN Huaixi[2,3], and LIANG Wanguo[2,3]****

1. College of Chemistry, Fuzhou University, Fuzhou 350108, China

2. Fujian Institute of Research on the Structure of Matter, Chinese Academy of Sciences, Fuzhou 350108, China

3. Fujian Science & Technology Innovation Laboratory for Optoelectronic Information of China, Fuzhou 350108, China

(Received 23 March 2023; Revised 26 July 2023)

This study investigates the fabrication process of Zn-diffused ridge waveguides in periodically poled magnesium-doped lithium niobate (PPMgO: LN). A controlled variable method is used to study the effects of diffusion temperature, diffusion time, ZnO film thickness, and barrier layer thickness on the surface domain depolarization and waveguide quality of PPMgO: LN. A special barrier layer is proposed that can automatically lift off from the sample surface, which increases the depth of Zn doping and reduces the surface loss of the waveguide. By optimizing the process parameters, we fabricate Zn-diffused PPMgO: LN ridge waveguides with a length of 22.80 mm and a period of 18.0 μm. The above waveguides can make a second harmonic generation (SHG) at 775 nm with an output power of 90.20 mW by a pump power of 741 mW at 1 550 nm. The corresponding conversion efficiency is 3.160%/W·cm^2, and the waveguide loss is approximately 0.81 dB/cm. These results demonstrate that high-efficiency devices can be obtained through the fabrication process described in this paper.

Document code: A **Article ID:** 1673-1905(2024)01-0012-6

DOI https://doi.org/10.1007/s11801-024-3051-3

Wavelength converter devices based on quasi-phase matching (QPM) technology for periodically poled lithium niobate (PPLN) channel waveguides can efficiently and compactly obtain laser light sources at wavelengths that are not available in the traditional laser market. Meanwhile, to meet the requirements of high integration and high conversion efficiency, the fabrication of PPLN waveguide devices is of utmost importance. Currently, the main fabrication methods of lithium niobate (LN) waveguides include annealed proton exchange[1], Ti diffusion[2], direct bonding and grooving[3], etc. Annealed proton exchange waveguides only support specific polarization modes and the application scenarios are limited. Ti diffusion LN waveguides support TE/TM dual polarization. Due to the doping of Ti, the optical damage resistance of the waveguide is reduced, which makes it unsuitable for high-power (≥200 mW) pumping devices. While high-power laser output has been achieved, the direct bonding process requires high-precision bonding and polishing equipment, which is complex and costly to manufacture.

Recently, the newly developed Zn-diffused LN waveguide[4] can not only support the TE/TM dual polarization mode, but also has strong optical damage resistance. In 2020, LEWIS et al[5] generated 2.5 W of 1 560—780 nm second harmonic generation (SHG) through a 4.0-cm-long ridge waveguide, corresponding to a pump power of 3.37 W. The normalized conversion efficiency of the device is 1.376%/W·cm^2. Refs.[5—12] prove the practicality of Zn diffusion waveguides. Due to their high economic benefits and wide application scenarios, it is necessary to further explore simple, low equipment requirements, and higher conversion efficiency diffusion processes to obtain stable and suitable fabrication processes for enterprises.

Therefore, this paper aims to explore the low-cost, high-performance atmospheric pressures Zn diffusion process from scratch and strive to achieve the commercialization of Zn diffusion periodically poled magnesium-doped lithium niobate (PPMgO: LN) waveguides. It primarily addresses the issue that a single ZnO film cannot guarantee the depth of Zn doping and alleviates the problem of surface depolarization in the PPLN domain structure during high-temperature diffusion. We optimized the key parameters of the waveguide fabrication process and ultimately obtained a 775 nm frequency

* This work has been supported by the Self-deployment Project of Fujian Science & Technology Innovation Laboratory for Optoelectronic Information of China (No.2021ZZ104), the Fujian Province STS Project: Design and Key Technology Research of High-Precision Multi-Section (5-10) Lithium Battery Protection Chip (No.2020T3002), and the Fujian Province STS Project: Research on the Preparation and Industrialization Technology of Volume Holographic Grating based on Photorefractive Glass (No.2022T3012).

** E-mails: hxchen@fjirsm.ac.cn; wgl@fjirsm.ac.cn

doubling output at the 100 mW level.

The crystal used in this experiment is a 7.62-cm 0.50-mm-thick single domain *Z*-cut MgO: LN wafer. We fabricated the designed polarization electrode pattern on the −*Z* plane of an MgO: LN wafer using photolithographic technology. At ~175 °C, a high-voltage pulse of ~1.8 kV was applied to the liquid electrode, achieving periodic domain inversion. The polarization period ranges from 17.90 μm to 18.50 μm. These PPLN period ranges can achieve frequency-doubling conversion from 1 550 nm to 775 nm.

As shown in Fig.1, we cut the wafer into a size of 3.00 mm (*W*) × 24.00 mm (*L*) sample, and clean the +*Z* surface of the crystal. We deposited 150 nm ZnO thin films on the +*Z* surface of LN by magnetron sputtering coater. Afterward, a barrier layer structure was deposited on the ZnO film using an electron beam evaporation coating machine. This structure is composed of 50 nm SiO_2, 50 nm Zn, 50 nm SiO_2, 150 nm Cr, and 50 nm SiO_2 films in sequence. Place the above samples in a tubular annealing furnace. In an oxygen-rich atmosphere, raise the sample to a temperature range of 900—1 000 °C at a heating rate of 14—16 °C/min. The diffusion time is 3—7 h. After the time is up, the sample will naturally cool to room temperature. The barrier layer will automatically fall off after the sample cools down. Occasionally, a small amount of metal particles remain on the surface of the sample. This can be removed with a 20% $(NH_4)_2Ce(NO_3)_6$ aqueous solution. On the diffusion surface of the sample, ridge waveguides with a depth greater than 35 μm and width ranging from 6 μm to 13 μm are fabricated using a precision grinding wheel grooving technology. Finally, the Zn diffused PPMgO: LN ridge waveguide was obtained through end surface polishing[13]. Fig.2 shows the polished end face of the ridge waveguide. The end faces of the samples in this paper refer to this figure.

The domain depolarization problem caused by high-temperature Zn diffusion PPLN seriously affects the wavelength conversion performance of the waveguide. To address this issue, we investigated the relationship between depolarization depth and diffusion conditions. We cut the Zn diffusion sample along the *X*-axis of the crystal. Afterward, polish the *Y*-section of the sample and corrode it with the HF solution. Finally, place the sample under a microscope and calculate the depolarization depth through software. As shown in Fig.3, we define the surface depolarization phenomenon in different regions. This includes a complete depolarization region, a depolarization region dominated by Zn doping, and a polarization-holding region. It can be seen in the figure that the periodic domain structure in the fully depolarized region has completely disappeared. The region has returned to its initial single-domain state. The polarization-holding region maintains the original periodic domain structure of the polarized crystal. The periodic domain structure boundaries in the remaining regions undergo some degree of deformation. Analyze the impact of depolarization on waveguide performance by testing the size of each region. This can explore an appropriate range of depolarization depth. In addition, this paper directly analyzes the mode spot quality of waveguide output using the through-light method. And the *Y*-direction diameter (D4σY) of the beam was calculated using an instrument. Then quantitatively analyze the range of refractive index changes in the waveguide based on the size of D4σY.

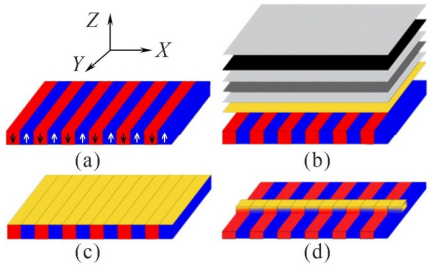

Fig.1 Process steps for preparing Zn diffusion PPMgO: LN ridge waveguide: (a) Periodically poling of LN crystal; (b) Depositing ZnO film by magnetron sputtering, and then depositing SiO_2, Zn, SiO_2, Cr and SiO_2 films with different thicknesses by electron beam evaporation as barrier layers; (c) Zn-diffusion at high temperature; (d) Fabricating ridge waveguide by precision dicing-saw, and polishing the end face

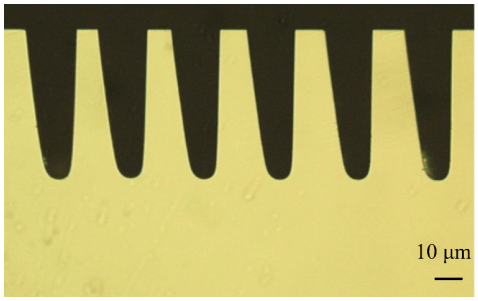

Fig.2 Partial view of the waveguide end face under a microscope

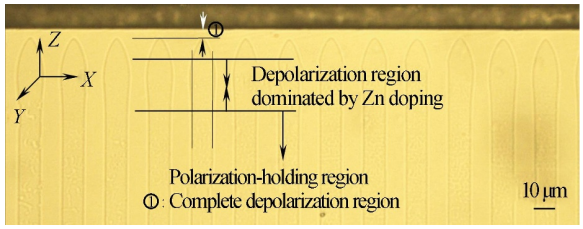

Fig.3 Schematic diagram of Zn diffused PPMgO: LN surface domain depolarization observed under an optical microscope (The figure defines the complete depolarization region, the depolarization region dominated by Zn doping, and the polarization-holding region)

Zn diffusion process parameters include diffusion temperature, diffusion time, thickness of ZnO film, etc. By changing the process parameters and fixing the waveguide ridge width (8—9 μm), we fabricated different

ridge waveguide samples. The 1 550 nm pump light is coupled into different waveguide samples through optical fibers and collimators. At the output end, a Spiricon LT665 beam profile analyzer is used to detect the mode spot quality of the waveguide output, and the D4σX, D4σY values measured by the instrument are recorded. Waveguide loss formula is

$$P_{out}=P_{in}\exp(-\alpha l), \quad (1)$$

where α is the loss coefficient, and the unit is cm^{-1}; l is the device length, and the unit is cm; P_{out} is the output power; P_{in} is the input power.

Use Eq.(1) to test and calculate the losses of different waveguides. We tested the SHG output power of each sample. Because the vast majority of samples do not have SHG output, we did not display the corresponding results. After completing the optical testing, we processed the sample through the acid corrosion method. Then measure the depths of the complete depolarization region, Zn-doped depolarization region, and total depolarization region using an optical microscope.

The process conditions include atmospheric pressure, the oxygen flow rate of 3 NL/min, ZnO thickness of 150 nm, SiO_2 thickness of 250 nm, and diffusion time of 300 min. The effects of different temperatures on depolarization depth, D4σY, and waveguide loss are shown in Fig.4 under the aforementioned conditions. The depolarization depth of Zn-doped samples must be greater than 10 μm to be measured. At 1 000 °C and diffusion time longer than 4 h, impurity atoms diffuse into the crystal interior due to the presence of a SiO_2 barrier layer, resulting in surface loss of the waveguide. At 1 000 °C and a diffusion time of ≥6 h, the samples are directly destroyed by the eutectic phase.

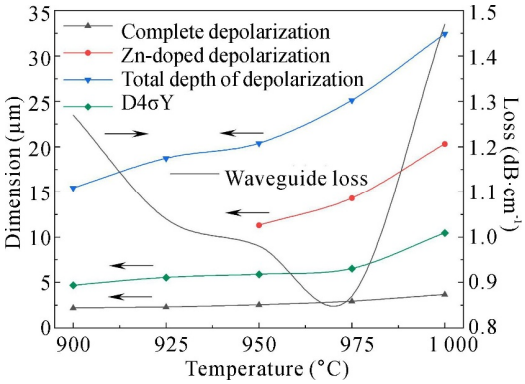

Fig.4 Effect of different temperatures on depolarization depth, D4σY and waveguide loss

The process conditions include atmospheric pressure, the oxygen flow rate of 3 NL/min, ZnO thickness of 150 nm, SiO_2 thickness of 250 nm, and diffusion temperature of 950 °C. The effects of different diffusion time on the depth of depolarization, D4σY, and waveguide losses are shown in Fig.5 under the aforementioned conditions. Under our experimental conditions, the waveguide does not transmit light when the diffusion time is less than 120 min. When the diffusion time exceeds 360 min, the waveguide losses increase significantly due to the diffusion of impurity atoms into the crystal. If the diffusion time or temperature is further increased, serious surface damage issues may arise due to the residual barrier layer, and even sample destruction may occur. Without a barrier layer, the waveguide is not practical. Since the depth of Zn doping is low, there will be no Zn-doped depolarization region. Furthermore, due to the volatilization of Li_2O, the degree of depolarization is enhanced. Therefore, based on the improved barrier layer structure, we continue to study the effects of ZnO film thickness and total barrier layer thickness on the performance of the waveguide. The change of the total barrier layer thickness is the accumulation of equal proportion changes in the thickness of each film layer.

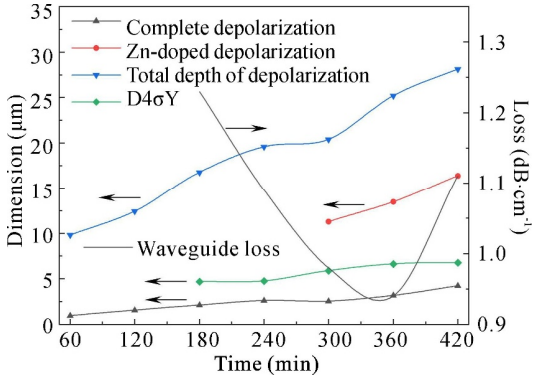

Fig.5 Effect of diffusing time on depolarization depth, D4σY and waveguide loss

The process conditions are as follows: atmospheric pressure, the oxygen flow rate of 3 NL/min, barrier layer with a thickness of 350 nm, diffusion temperature of 950 °C, and diffusion time of 300 min. The effects of different ZnO film thicknesses on depolarization depth, D4σY, and waveguide loss under the above conditions are shown in Fig.6. From the curves in the graph, it can be observed that the continuous increase in ZnO film thickness promotes deeper Zn doping, increases the D4σY value, and inhibits the escape of Li_2O. Based on the experimental observations, it can be concluded that the increase in ZnO film thickness significantly slows down the diffusion of impurity atoms into the crystal interior and the formation of eutectic problems, resulting in improved waveguide performance as shown in Fig.6. However, increasing the thickness of ZnO film may result in decreased film density and deteriorated performance of the barrier layer. Finally, when the ZnO film thickness exceeds 340 nm, the waveguide performance deteriorates.

The process conditions are as follows: atmospheric pressure, 3 NL/min oxygen flow rate, 300 nm ZnO, 950 °C diffusion temperature, and 300 min diffusion time. Under the above conditions, the effects of different

total film thicknesses of barrier layers on depolarization depth, D4σY, and waveguide loss are shown in Fig.7. From Figs.4—7, it can be seen that the gradual evaporation of Zn vapor leads to a significant decrease in the blocking ability of the composite barrier layer compared to the 250 nm SiO_2 film. This evaporation ensures the quality of the waveguide while significantly improving the surface smoothness of the sample after diffusion. This is an advantage that a single SiO_2 film barrier layer does not have. The waveguide losses in Figs.6 and 7 are smaller and better. However, when the total film thickness is >500 nm, the effect of automatic separation of the barrier layer deteriorates. The residual amount of the barrier layer reaches a certain level, which will also cause impurity atoms to diffuse into the interior of the crystal, resulting in waveguide loss. From the experimental results, it can be seen that the barrier layer can significantly promote the depth of Zn doping. This is beneficial for slowing down diffusion conditions and the degree of depolarization.

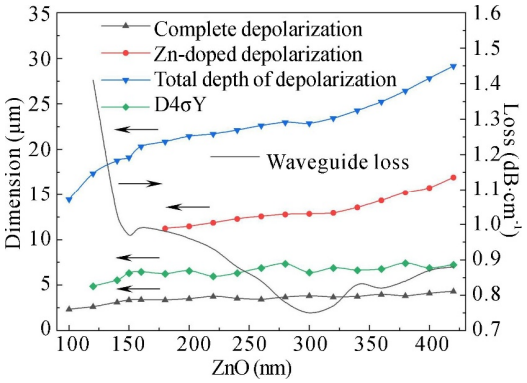

Fig.6 Effect of ZnO film thickness on depolarization depth, D4σY and waveguide loss

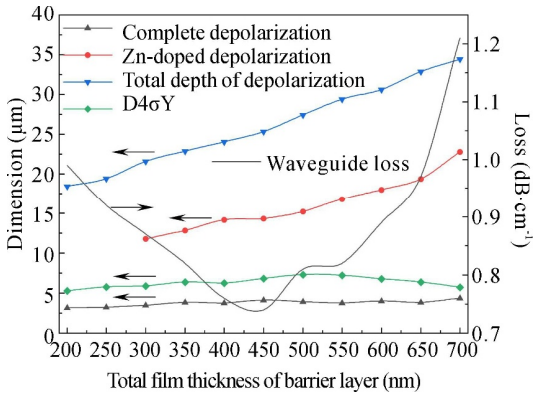

Fig.7 Effect of barrier film thickness on depolarization depth, D4σY and waveguide loss

From the results in Figs.4—7, it can be seen that Zn doping causes depolarization. The special barrier layer at 350—500 nm can effectively promote the depth of Zn doping and reduce surface loss. We should appropriately slow down the diffusion conditions to control the total depolarization depth <20 μm and ensure that the depth of the Zn doped depolarization region is >10 μm. It is possible to obtain high-performance ZnO diffusion PPMgO: LN waveguides.

We deposited a 300 nm ZnO film and a 450 nm special barrier layer on the *Z*-plane of the crystal. The sample waveguide was obtained under diffusion conditions of 950 °C and 5 h. We install the waveguide on a temperature-controlling stove and couple the broadband beam into the waveguide through optical fibers and collimators. Measure the second harmonic spectrum of the waveguide through a spectrometer. Find the wavelength corresponding to the strongest second harmonic through the spectrogram. As shown in Fig.8, the peak wavelength corresponding to a ridge waveguide is 769.17 nm. Multiply this value by 2, and add the narrow linewidth light source device wavelength drift value of 0.76 nm. The center wavelength of the waveguide obtained is 1 539.10 nm. Set the output wavelength of a narrow linewidth light source. The light source is connected to a 5 W erbium-doped fiber amplifier through optical fibers. The amplified light is coupled into the ridge waveguide through a collimator. The pump light is removed by an infrared filter to obtain the frequency-doubling light output by the waveguide. Finally, use an optical power sensor to measure the power value of the frequency-doubling light (see Fig.9).

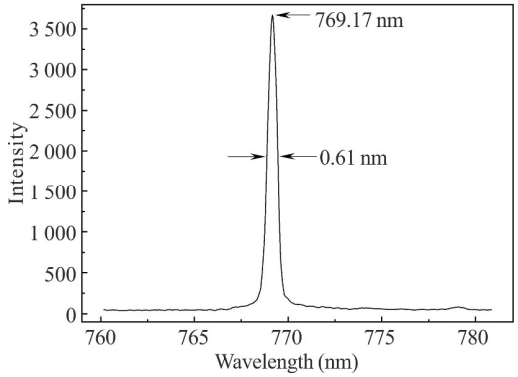

Fig.8 Measured peak second harmonic wavelength of the waveguide using a broadband light source

In the experiment, we did not rule out the Fresnel reflection loss at each end face of the waveguide. Using the testing device shown in Fig.9, we measured the maximum frequency-doubling output power of the waveguide TM mode at a working temperature of 27.4 °C, which is 90.2 mW. After fixing the testing device and removing the waveguide, the pump power corresponding to the waveguide input end was measured to be 741 mW. The waveguide length is 2.28 cm. The normalized conversion efficiency of the waveguide is about 3.16%/W·cm^2, which is still some distance from commercialization. Tab.1 shows the literature reports of similar waveguides. Under the same wavelength and input power, the relationship between the waveguide frequency doubling power and the quasi-phase-matching temperature is measured by adjusting the temperature, as shown in

Fig.10. The test curve in the figure and the sinc^2 function are approximately fitted. The waveguide ridge width is 8.87 μm. The measured and calculated loss of the waveguide is approximately 0.81 dB/cm.

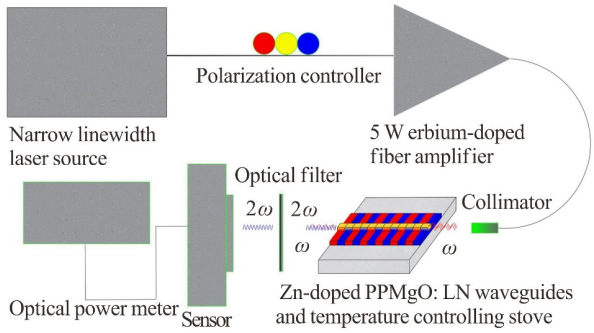

Fig.9 Waveguide output power measurement device

Tab.1 PPLN waveguide CW SHG power and efficiencies for the C-band (Efficiencies have been recalculated to be normalized with power only; NR: Not reported)

Waveguide type	η_{norm}	Anti-reflection	P_{max}
Zn: PPLN[5]	1.376%/W·cm^2	AR	2.5 W
Zn: PPLN[6]	6.3%/W·cm^2	AR	1 W
Bonding PPLN[14]	22%/W·cm^2	AR	1 W
Ti: PPLN[15]	0.986%/W·cm^2	NR	9 mW
RPE PPLN[16]	25%/W·cm^2	NR	1 W

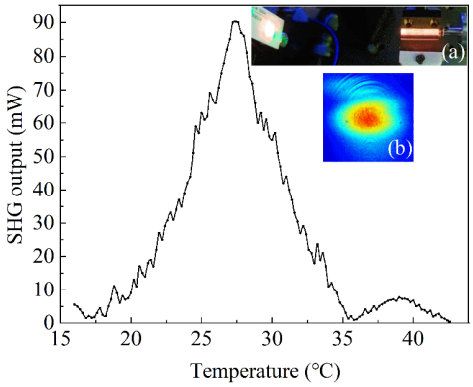

Fig.10 Relationship between SHG power and QPM temperature in Zn-diffused PPMgO: LN waveguides: (a) An actual photo of the waveguide testing process; (b) Spot of the frequency-doubled light generated by the waveguide

This paper investigates the effects of diffusion temperature, diffusion time, ZnO film thickness, and the total thickness of special barrier layers on the waveguide loss, beam diameter, and surface depolarization of Zn diffusion PPLN. We also studied the relationship between the size of the depolarization region and the performance of the waveguide and provided a reference range for the depolarization size corresponding to the waveguide with a conversion efficiency of 3.16%/W·cm^2. There are few literature reports on the Zn diffusion PPLN process using the barrier layers method. We have innovatively proposed a barrier layer structure that can automatically separate from the diffusion surface. This structure perfectly solves the problems of Zn doping depth, surface depolarization, and impurity atom diffusion, and successfully obtains a 100 mW level Zn diffusion PPLN wavelength conversion waveguide. Optimizing the relevant processes is expected to further improve conversion efficiency.

Ethics declarations

Conflicts of interest

The authors declare no conflict of interest.

References

[1] YUAN J, DU J, LIU J, et al. Arayed-waveguide-grating based on proton exchange and etching combined fabrication over bulk lithium-niobate substrate[C]//2022 IEEE 24th International Workshop on Multimedia Signal Processing (MMSP), September 26-28, 2022, Shanghai, China. New York: IEEE, 2022: 1-4.

[2] NIU Y, YAN X, CHEN J, et al. Research progress on periodically poled lithium niobate for nonlinear frequency conversion[J]. Infrared physics & technology, 2022: 104243.

[3] TAKUSHI K, TAKESHI U, SHIMPI S, et al. Over-30-dB gain and 1-dB noise figure phase-sensitive amplification using a pump-combiner-integrated fiber I/O PPLN module[J]. Optics express, 2021, 29(18): 28824-28834.

[4] CHEN Z Y, CHENG J X, CHEN H X, et al. High performance Zn diffused Mg doped LN crystal ridge waveguide devices[J]. Journal of synthetic crystals, 2022, 51(11): 1823.

[5] LEWIS G C, SAM A B, ALAN C G, et al. CW demonstration of SHG spectral narrowing in a PPLN waveguide generating 2.5 W at 780 nm[J]. Optics express, 2020, 28(15/20): 21382.

[6] BERRY S A, CARPENTER L G, GRAY A C, et al. Zn-indiffused diced ridge waveguides in MgO: PPLN generating 1 watt 780 nm SHG at 70% efficiency[J]. OSA continuum, 2019, 2(12): 3456-3464.

[7] LU M, CORIN B E G, KATIA G, et al. High conversion efficiency single-pass second harmonic generation in a zinc-diffused periodically poled lithium niobate waveguide[J]. Optics express, 2005, 13(13): 4862.

[8] ALAN C G, SAM A B, LEWIS G C, et al. Upconversion detection of 1.25 Gb/s mid-infrared telecommunications using a silicon avalanche photodiode[J]. Optics express, 2020, 28(23/9): 34279.

[9] ALAN C G, JONATHAN R C W, LEWIS G C, et al. Zinc-indiffused MgO: PPLN waveguides for blue/UV generation via VECSEL pumping[J]. Applied optics, 2020, 59(16/1): 4921.

[10] ALAN C G, SAM A B, LEWIS G C, et al. Investigation of PPLN waveguide uniformity via second harmonic generation spectra[J]. IEEE photonics technology letters, 2019, 32(1): 1041-1135.

[11] CARPENTER L G, BERRY S A, BANNERMAN R H S, et al. ZnO indiffused MgO: PPLN ridge waveguides[J]. Optics express, 2019, 27(17): 24538-24544.

[12] GRAY A C, CARPENTER L G, BERRY S A, et al. Development of periodically poled lithium niobate zinc-indiffused ridge waveguides at blue wavelengths[C]//2019 Conference on Lasers and Electro-Optics Europe & European Quantum Electronics Conference (CLEO/Europe-EQEC), June 23-27, 2019, Munich, Germany. New York: IEEE, 201: 1-1.

[13] CARPENTER L G, BERRY S A, GAWITH C. Ductile dicing of $LiNbO_3$ ridge waveguide facets to achieve 0.29 nm surface roughness in single process step[J]. Electronics letters, 2017, 53(25): 1672-1674.

[14] PECHEUR V, PORTE H, HAUDEN J, et al. Watt-level SHG in undoped high step-index PPLN ridge waveguides[J]. OSA continuum, 2021, 4(5): 1404-1414.

[15] SHANTANU P, BIJOY K D, WOLFGANG S. Photorefractive damage resistance in Ti: PPLN waveguides with ridge geometry[J]. Applied physics B, 2015, 120(4): 737-749.

[16] SUNTSOV S, RUTER C E, BRUSKE D, et al. Watt-level 775 nm SHG with 70% conversion efficiency and 97% pump depletion in annealed/reverse proton exchanged diced PPLN ridge waveguides[J]. Optics express, 2021, 29(8): 11386-11393.